Link to publication

University of Bath

Alternative formats

If you require this document in an alternative format, please contact:
openaccess@bath.ac.uk

A new microfluidic pressure-controlled Field Effect Transistor (pFET) in digital fluidic switch operation mode

Nikolaos Vourdas[a,c], Despina C. Moschou [b], Konstantinos A. Papadopoulos[c], Dimitrios Davazoglou[a], Vassilis N. Stathopoulos[c]

[a] *Institute of Nanoscience and Nanotechnology, NCSR Demokritos, Aghia Paraskevi 15310, Attiki, Greece*

[b] *Centre for Advanced Sensor Technologies, Electronic and Electrical Engineering, University of Bath, BA2 7AY, Bath, UK*

[c] *School of Technological Applications, Technological Education Institute of Sterea Ellada, Psachna campus, 34400, Evia, Greece*

Abstract

Lab-on-Chip is currently considered the technology with the potential to revolutionize future biochemical analysis, providing miniaturized, low-reagent volume microchips as an alternative to traditional benchtop analysis. Automated control of droplet flow is currently a key objective in microfluidics research, aiming for droplet logic microfluidic circuits. To this end, microfluidic research has been following the electronics paradigm, with several digital fluidic components being demonstrated towards the realization of digital fluidic circuits for automated liquid control and delivery. In this work we introduce a new concept of microfluidic pressure controlled field-effect transistors (pFETs), towards droplet logic operations. Using a fluidic with porous and hydrophobic walls, the inherently pinned plug depins by pressure application through the porous wall (backpressure), thus enabling the actuation and the downward transportation of the plug due the action of gravity. This concept resembles the logic operation of a metal–oxide–semiconductor field-effect transistor (MOSFET). The pFET operating parameters are thus defined in a manner analogous to MOSFET digital switches and their dependence on the channel width is studied also for the first time. The successful operation of pFET devices for droplet logic operation is verified in continuous ON/OFF cycles, achieving OFF-ON and ON-OFF switching times under 1 sec (0.864 s and 0.841 s respectively) and therefore promising rapid liquid switching times, comparable to electronic circuit ones.

1. Introduction

Lab-on-Chip refers to a technology aspiring to miniaturize biochemical analysis laboratories onto few centimeter microchips, and thus revolutionize the current healthcare diagnosis practice globally [1]. This technology promises highly portable diagnostic systems, while at the same time benefitting from rapid analysis time and reduced reagent costs; all of these advantages are ascribed to the miniaturization of the liquid reagent transport networks, also known as microfluidics [2, 3]. Nonetheless, in order to achieve the full potential of microfluidic devices, automated handling and dispensing of the relevant fluid samples at a microchip level is required [4]. While several approaches are being explored for assay automation, mostly exploiting external control systems, there is not yet an established solution for automated on-chip liquid handling.

Microfluidics research has followed historically the advancements in the field of microelectronics and microsystems, with the latter providing mature concepts, technologies and tools to the former, and thus inspiring novel microfluidic structures, smart materials, fabrication methods and embedded systems concepts for automated liquid control in small scales [5-10]. Currently, the convergence of established low cost microelectronic technology with microfluidic applications is at the forefront, aspiring to autonomous, fully integrated Lab-on-Chip microsystems [11-13].

However, this dependence has been working also reversibly. The liquids being transferred through microfluidics, include chemical, biochemical or biologic information. By manipulating liquid droplets with such information along a fluidic, one can actually perform logic operations analogous to digital electronics; in the latter case electronic packages of information (bits) are exploited, whilst in the former liquid packages (droplets). The potential of this approach for implementing fully autonomous assays, via "droplet logic operations" was identified by Prakash et al [14] and has since attracted much attention. The most integrated approach has been provided by G. Katsikis et al in 2015 [15]; a platform using a rotating magnetic field enabling synchronous manipulation of ferrofluid droplets was presented,

thus facilitating autonomous parallel droplet manipulation, analogous to the scaling seen in digital electronics. OR/AND logic gates, universal XOR/AND and XOR/NAND gates, flip-flops, etc were demonstrated through droplet movement, predicting "new avenues in mesoscale material processing".

But this is not the only example. Droplet logic computations have been recently performed by Woodhouse and Dunkel and presented as active matter logic [16, 17]. Droplet logic gates have been prepared [18-20]. Fluidic diodes have been demonstrated either through a membrane [21], along a micro channel [22], or along a specially designed surface with re-entrant geometry [23]. The group of Prof. Ras [24] performed computation with droplets acting as bits of information. Optically displayed information has been stored and erased reversibly in superhydrophobic surfaces with dual scale roughness by means of over- or under- pressure [25]. Switches and liquid transistors with liquid metals have been demonstrated by moving droplets with electricity [26]. In the nanoscale, the term field effect fluidics has been used by Prakash and Gershenfeld [27]. Diodes [28, 29], transistors [30], and pertinent logical devices [31-35] have been fabricated and characterized thoroughly, employing either electrical, optical, or mechanical biases as control signals. Very recently, an electrically driven thyristor, acting as an electrically controlled valve, has been demonstrated in paper microfluidic devices [36]. Incorporating such automated liquid control in porous, paper structures, will allow the automation of more complex paper-based biochemical assays than currently demonstrated, and thus fully exploit paper-based device potential as a low-cost diagnostic technology.

In this work we introduce the concept of a microfluidic pressure-controlled field-effect transistor (pFET), exploiting the channel wall porosity and hydrophobicity to achieve digital fluidic switch operation. The device characteristics are defined and extracted for various channel widths, in a manner analogous to microelectronic metal-oxide-semiconductor field effect transistor (MOSFET) devices, i.e. critical backpressure (ΔP_{cr}) ≈ threshold voltage (V_{th}), ON-state flow rate (Q_{sat}) ≈ ON-state drain current (I_{sat}), while its operation in continuous ON/OFF operation was evaluated.
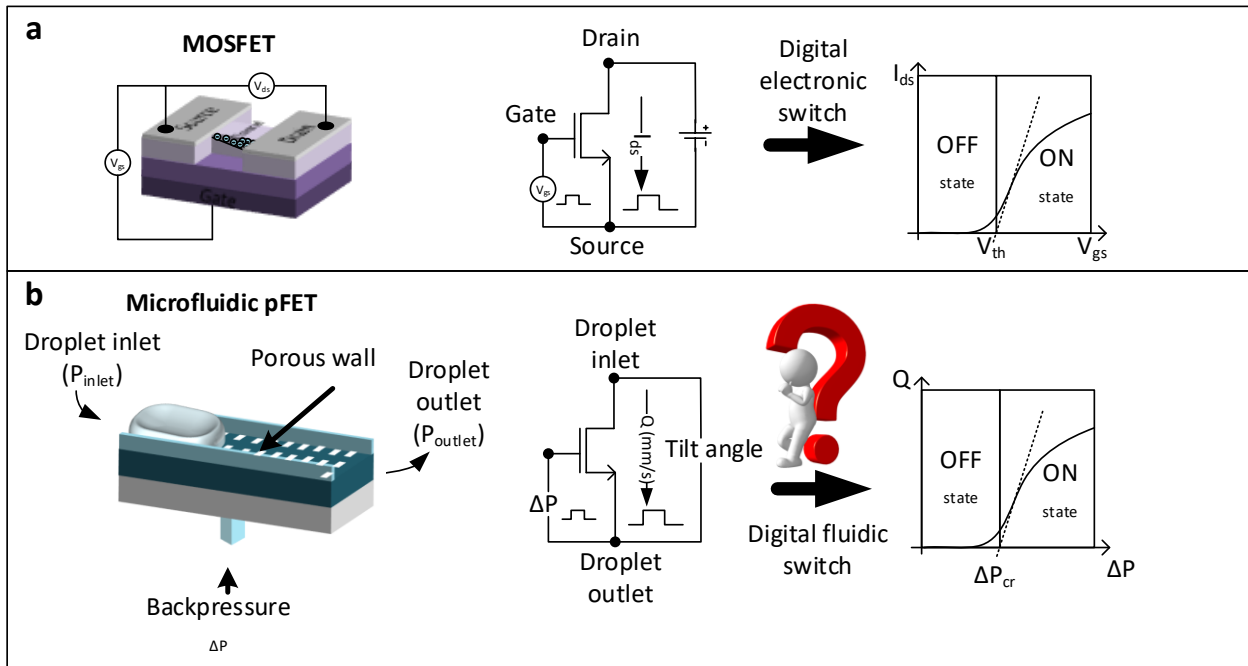
Fig. 1: (a) Schematic of a MOSFET device, circuit model and I-V characteristic and (b) Schematic of the microfluidic pFET conceptual analogous, electronic analogous model and Q-ΔP characteristic

Experimental

For the fabrication of the pFET device, commercially available honeycomb-type cellular ceramics of various cells per inch (cpsi) values were used. Such honeycombs are manufactured by mechanical extrusion, drying, de-binding and a sintering step. Typical cordierite ($Al_4Mg_2Si_5O_{18}$) ceramic honeycombs, with open unidirectional channels and square sharing walls, were used. The honeycombs were cut and machined to the required dimensions and geometry, leaving a central channel open on the top face. This channel after dry surface modification, to render the porous surfaces hydrophobic, serves as the fluidic channel [37-41]. Similarly, porous and hydrophobic structures prepared by alternative routes, such as 3d-printing may also be used. In all cases in this study deionized water was used to form the liquid plug.

All applied pressure values were measured using the KIMO MP 200HP manometer with 2 mbar accuracy.

2. Results and discussion

The basic operating principle of a field effect transistor (FET) in a digital switch mode (Fig. 1a) involves controlling the source and drain electrical current (I_{ds}) between cut-off ($I_{ds}=0$, OFF state) and saturation ($I_{ds}=I_{ds,sat}$, ON state) *via* the gate-source potential (V_{gs}).

For the pFET analogous we study in this work, the basic operational principle is the following: In a fluidic channel there is one "source" where the liquid plug is introduced (droplet inlet) and one "drain" where the plug will flow to (droplet outlet) (see Fig.1b for the outline, Fig.2a for a schematic representation and Fig.2b for photos during actual operation). The fluidic is titled so as the droplet outlet is at lower height and therefore lower pressure, due to the gravitational forces, i.e. P_{inlet}-P_{outlet}>0. The fluidic channel has porous (depicted as white holes in Fig.1b and seen in the SEM image in Fig.2c) and hydrophobic walls that are inherently sticky and therefore the plug is pinned and does not flow to the droplet outlet spontaneously, even though is titled and the inlet-outlet pressure gradient is positive

(Fig.2a(i)). However upon a backpressure application, namely a gas pressure applied through the walls, gas flow through the walls and the plug depins and is therefore actuated and flows along the channel (Fig.2a(ii)) downwards to the droplet outlet (Fig.2a(iii)).

plug velocity can be controlled by the backpressure value and hence in the microfluidic pFET device we study here (Fig. 1b) we control the liquid flow Q, from the droplet inlet to the outlet, between no flow ($Q=0$, OFF state) and maximum flow ($Q=Q_{sat}$, ON state) similarly to the operation of a MOSFET. The saturation drain-source current ($I_{ds,sat}$) value in
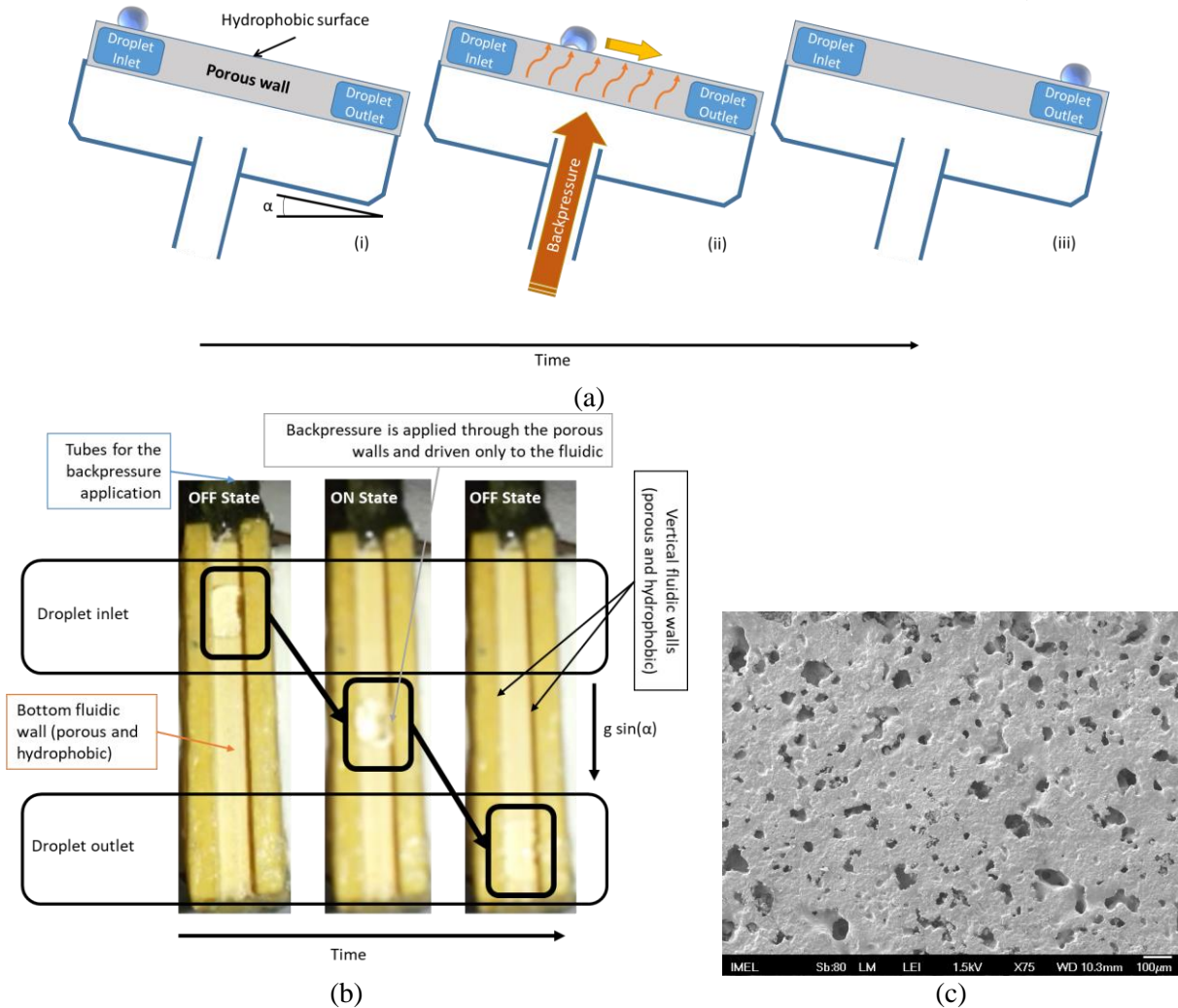

(a)

(b)

(c)

Fig. 2: a) Schematic representation of the operation principle of the pFET (i) A droplet or a plug is introduced in the droplet inlet and pins to the surface (OFF state), (ii) Backpressure is applied leveraging droplet depinning (ON state) and (iii) the droplet arrives at droplet outlet (OFF state). b) Snapshots from the actual operation of the pFET. The liquid plug introduced in the droplet inlet is actuated upon backpressure application and flows downwards to the droplet outlet. c) Top view SEM image of the porous and hydrophobic channel wall.

In this pFET device the droplet inlet to droplet outlet liquid flow (Q) is enabled only by the application of the backpressure (ΔP), which acts as gate-source potential analogue, and consequently the device is pressure-controlled. As will be shown below, the

MOSFETs can be modulated by the drain to source potenial (V_{ds}). In our pFET device (Table I), we control the flow Q by tilting it perpendicularly to the channel area, thus modulating the inlet (P_{inlet}) and outlet (P_{outlet}) pressure gradient caused by the action

of gravity. The transition between the OFF and ON states in MOSFETs is defined by the threshold voltage V_{th} value, which is calculated by linear extrapolating the I_{ds}-V_{gs} transfer characteristics. In this work we explore the possibility to apply a similar analysis to obtain a critical backpressure (ΔP_{cr}) for our microfluidic pFET devices.

Table. I: MOSFET and microfluidic pFET performance parameter analogy.

MOSFET	Microfluidic pFET
Gate-Source potential V_{gs}	Backpressure ΔP
Threshold voltage V_{th}	Critical backpressure ΔP_{cr}
Drain-Source potential V_{ds}	Inlet-outlet pressure gradient P_{inlet}-P_{outlet}
Drain-Source current I_{ds}	Channel flow rate Q
ON region saturation current $I_{ds,sat}$	ON region maximum flow rate Q_{sat}

In Fig.2b we provide snapshots of the pFET during operation. Initially the plug is introduced in the droplet inlet region where it pins. Below the bottom fluidic wall and next to the vertical fluidic walls, are channels enabling the backpressure application, only towards the fluidic. The gas supply for the backpressure is provided by small tubes, seen in the upper side of Fig.2b. Upon backpressure application through the porous and hydrophobic walls the plug depins and flows downwards to the droplet outlet. In the middle of Fig.2b, we show the plug during it's movement. When the plug arrives at the droplet outlet region the backpressure may be closed back again until another one plug comes to the droplet inlet region.

The operation of our pFET is based mainly on two properties of the fluidic walls. The first one being its porosity and the second its hydrophobicity.

In Fig.2c we a SEM image of the channel wall is reported showing the porous distribution. Pores with diameter up to 70-80 um can be identified along with smaller ones with diameters less than 30 um. As shown in a previously work [40], this particular pore distribution enables for backpressure values of the order of few mbar, which are appropriate for the operation of the pFET device with low energy consumption.

To avoid liquid imbibition the porous surface shall be hydrophobic. In the case studied herein, the static contact angle is higher than 120 deg.'s with the advancing contact angle being higher than 130 deg.'s

The above described pore structure and contact angle proved to be adequate for the proper operation of our device for the case of DI water (we note at this point that within this study only DI water was tested).

An advantageous characteristic of our pFET is that there is no need to attain superhydrophocity for its proper operation. It is noted that to obtain superhydrophobic surfaces special fabrication steps would be needed and the devices finally obtained would be subject to ageing and durability decline [42].

The flow Q between droplet inlet and droplet outlet was measured from video snapshots in microfluidic pFET devices, as the ones depicted in Fig. 2a, for various channel widths (0.8 – 3.3 mm) and plotted in relation to the applied ΔP value (Fig. 3), with a close to zero tilt angle.
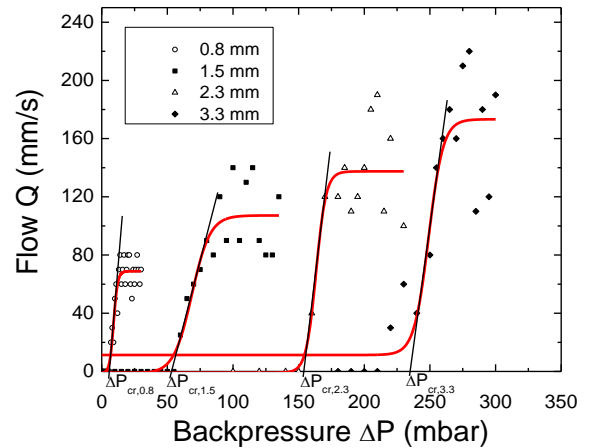

Fig. 3: Flow Q vs. backpressure ΔP applied on fluidics with various widths (0.8, 1.5, 2.3 and 3.3 mm) for a 20 ul plug. [Close to zero tilting].

It can be observed that indeed we can replicate satisfactorily MOSFET transfer characteristics for all characterized microfluidic pFETs, clearly distinguishing between OFF and ON states, however with large fluctuations in ON state Q_{sat} values. For all channel widths there is a clear transition area between OFF and ON, allowing us to apply the MOSFET linear extrapolation analysis to calculate the critical backpressure ΔP_{cr} value for each device. Analogous to MOSFETs, we can also clearly observe a linear increase of Q_{sat} with channel width. In wider channels, larger backpressure is needed to reach the

ON-state, entailing lower droplet/wall friction and thus achieving larger flow-rates.

In Fig. 4 we plot the calculated ΔP_{cr} as a function of the channel width, W, so as to investigate in more detail the observed narrow width effect in microfluidic pFET devices. It is evident that the channel width in the studied range (0.8 – 3.3 mm) plays an important role in the device ΔP_{cr} value, with the required pressure to transition from OFF to ON state decreasing with decreasing channel width. In Silicon on Insulator (SOI) MOSFETs such narrow width effects are frequently observed [43] and ascribed mainly to channel edge dopant segregation [44]. In the case of pFETs this is attributed to the fact that as the channel width increases the length of the plug (L) decreases and therefore the gravitational pressure favouring liquid flow ($\rho g L sin(\alpha)$) decreases, thus necessitating higher backpressure values [37].
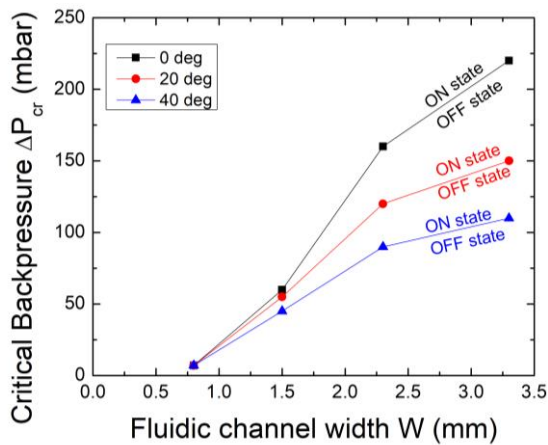

Fig. 4: Critical backpressure ΔP_{cr} vs. fluidic channel width W for a 20 ul plug volume.

As expected, ΔP_{cr} is reduced with increasing tilt angle, since the inlet-outlet pressure field (P_{inlet} - P_{outlet}) is increased, and thus less backpressure ΔP is required in the gate to enable liquid flow. This effect is more pronounced in wider devices.

Having characterized our pFET digital flow switch in terms of applied backpressure required to reach ON-state, we carried on to identify its performance with respect to switching time between OFF and ON state, sequentially applying $\Delta P=0$ mbar and ΔP_{cr} backpressure pulses at the gate (Fig. 5). The

variations of Q at the ON state depicted in Fig.5 are associated to the underlying mechanisms of actuation and mobility manipulation using backpressure. As have been studied both experimentally and numerically for flat and open surfaces [38], as well as for closed channel fluidics [45] the velocity of the front and back faces of the plug upon backpressure application is not constant. The plug undergoes various and complex shape deformations, and therefore does not exhibit a smooth movement. These shape deformations are reflected as flow variations.
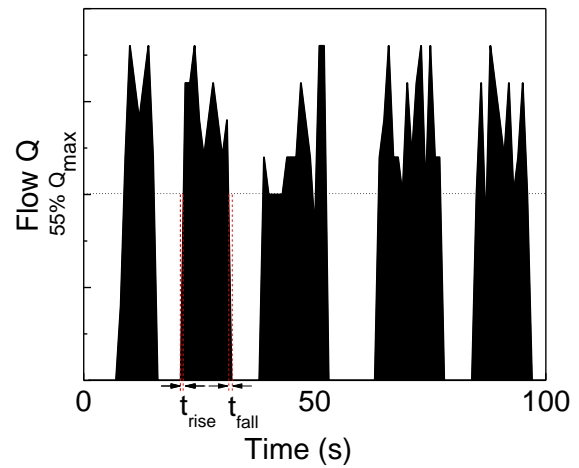

Fig. 5: OFF/ON switching cycles for a microfluidic pFET (L=0.8 mm, W=0.8 mm) and for a 20 μl plug.

The switching rise (t_{rise}) and fall (t_{fall}) times were measured to be t_{rise}= 0.864 ± 0.442 s, t_{fall} = 0.841 ± 0.458 s (N=10 ON/OFF cycles); t_{rise} is defined as the time between critical backpressure application and a flow Q at 55% of its maximum (55%Q_{max}), and t_{fall} as the time elapsed between 55%Q_{max} and Q=0 mm/s. The relatively large uncertainty observed for t_{rise} and t_{fall} is attributed to the different shape deformations undergone by the droplet upon backpressure application, resulting in a variation of the time required for the droplet to transition from the OFF (Q=0 mm/s) to the ON state (Q=55%Q_{max}) and vice versa.

4. Conclusions

In this paper we have introduced the concept of a microfluidic pressure-driven field-effect transistor (pFET), exploiting the porosity and hydrophobicity of the microfluidic channel walls for liquid actuation and mobility manipulation towards droplet logic operations. We demonstrated that the suggested microfluidic device, the pFET, can be exploited as a digital flow switch, exhibiting switching characteristics analogous to the MOSFET switch. The critical switching parameters for the device were defined (ΔP_{cr}, Q_{sat}, t_{rise}, t_{fall}) and the average ON/OFF switching times were calculated to be t_{rise}= 0.864 s and t_{fall}= 0.841 s. We observed a substantial effect of channel width on ΔP_{cr} and Q_{sat} values, demonstrating the analogy between microelectronic and microfluidic transistor operation and thus enabling the development of pFET logic gates and digital circuitry. The theoretically anticipated decrease in ΔP_{cr} with respect to increasing inlet-outlet pressure was verified through increasing the tilt angle perpendicular to the channel. Future work enabled by the presented results involves fabrication and characterization of more complex pFET circuits and implementation of this concept in alternative porous substrates like hydrophobic paper, allowing fluidic automation in complex paper-based assays unachievable until now.

References

1. Whitesides, G.M., *The origins and the future of microfluidics.* Nature, 2006. **442**(7101): p. 368-373.
2. Moschou, D., et al., *All-plastic, low-power, disposable, continuous-flow PCR chip with integrated microheaters for rapid DNA amplification.* Sensors and Actuators B: Chemical, 2014. **199**: p. 470-478.
3. Temiz, Y., et al., *Lab-on-a-chip devices: How to close and plug the lab?* Microelectronic Engineering, 2015. **132**: p. 156-175.
4. Niu, X., F. Gielen, and J.B. Edel, *A microdroplet dilutor for high-throughput screening.* Nature chemistry, 2011. **3**(6): p. 437-442.
5. Bhattacharjee, N., et al., *The upcoming 3D-printing revolution in microfluidics.* Lab on a Chip, 2016. **16**(10): p. 1720-1742.
6. Gogolides, E., K. Ellinas, and A. Tserepi, *Hierarchical micro and nano structured, hydrophilic, superhydrophobic and superoleophobic surfaces incorporated in microfluidics, microarrays and lab on chip microsystems.* Microelectronic Engineering, 2015. **132**: p. 135-155.
7. Mavraki, E., et al., *A continuous flow µPCR device with integrated microheaters on a flexible polyimide substrate.* Procedia Engineering, 2011. **25**(0): p. 1245-1248.
8. Ellinas, K., A. Tserepi, and E. Gogolides, *Superhydrophobic, passive microvalves with controllable opening threshold: exploiting plasma nanotextured microfluidics for a programmable flow switchboard.* Microfluidics and Nanofluidics, 2014. **7**(3): p. 1-10.
9. Vourdas, N., et al., *Plasma processing for polymeric microfluidics fabrication and surface modification: Effect of super-hydrophobic walls on electroosmotic flow.* Microelectronic Engineering, 2008. **85**(5): p. 1124-1127.
10. Vourdas, N., A. Tserepi, and E. Gogolides, *Nanotextured super-hydrophobic transparent poly (methyl methacrylate) surfaces using high-density plasma processing.* Nanotechnology, 2007. **18**(12): p. 125304.
11. Moschou, D. and A. Tserepi, *The lab-on-PCB approach: tackling the [small mu]TAS commercial upscaling bottleneck.* Lab on a Chip, 2017. **17**(8): p. 1388-1405.
12. Jebrail, M.J., et al., *Synchronized synthesis of peptide-based macrocycles by digital microfluidics.* Angewandte Chemie International Edition, 2010. **49**(46): p. 8625-8629.
13. Sesen, M., T. Alan, and A. Neild, *Droplet Control Technologies for Microfluidic High Throughput Screening (µHTS).* Lab on a Chip, 2017.
14. Prakash, M. and N. Gershenfeld, *Microfluidic bubble logic.* Science, 2007. **315**(5813): p. 832-835.
15. Katsikis, G., J.S. Cybulski, and M. Prakash, *Synchronous universal droplet logic and control.* Nature Physics, 2015. **11**: p. 588-596.
16. Woodhouse, F.G. and J. Dunkel, *Active matter logic for autonomous microfluidics.* Nature Communications, 2017. **8**.
17. Woodhouse, F.G., J.B. Fawcett, and J. Dunkel, *Information transmission, holographic defect detection and signal permutation in active flow networks.* arXiv preprint arXiv:1705.00589, 2017.
18. Cheow, L.F., L. Yobas, and D.-L. Kwong, *Digital microfluidics: Droplet based logic gates.* Applied Physics Letters, 2007. **90**(5): p. 054107.
19. Kou, S., et al., *Fluorescent molecular logic gates using microfluidic devices.* Angewandte Chemie International Edition, 2008. **47**(5): p. 872-876.
20. Zhou, B., et al., *Universal logic gates via liquid-electronic hybrid divider.* Lab on a Chip, 2012. **12**(24): p. 5211-5217.
21. Mates, J.E., et al., *The fluid diode: tunable unidirectional flow through porous substrates.* ACS applied materials & interfaces, 2014. **6**(15): p. 12837-12843.
22. Feng, J. and J.P. Rothstein, *One-way wicking in open micro-channels controlled by channel topography.* Journal of Colloid and Interface Science, 2013. **404**: p. 169-178.

23.   Li, J., et al., *Topological liquid diode.* Science advances, 2017. **3**(10): p. eaao3530.

24.   Mertaniemi, H., et al., *Rebounding Droplet-Droplet Collisions on Superhydrophobic Surfaces: from the Phenomenon to Droplet Logic.* Advanced Materials, 2012. **24**(42): p. 5738-5743.

25.   Verho, T., et al., *Reversible switching between superhydrophobic states on a hierarchically structured surface.* Proceedings of the National Academy of Sciences, 2012. **109**(26): p. 10210–10213.

26.   Wissman, J., M.D. Dickey, and C. Majidi, *Field-Controlled Electrical Switch with Liquid Metal.* Advanced Science, 2017.

27.   Prakash, S. and A. Conlisk, *Field effect nanofluidics.* Lab on a Chip, 2016. **16**(20): p. 3855-3865.

28.   Cheikh, M. and I. Lakkis, *Microfluidic transistors for analog microflows amplification and control.* Microfluidics and Nanofluidics, 2016. **20**(6): p. 1-24.

29.   Sochol, R.D., et al., *Microfluidic bead-based diodes with targeted circular microchannels for low Reynolds number applications.* Lab on a Chip, 2014. **14**(9): p. 1585-1594.

30.   Mo, J., et al., *Passive fluidic diode for simple fluids using nested nanochannel structures.* Physical Review E, 2016. **93**(3): p. 033101.

31.   Toepke, M.W., V.V. Abhyankar, and D.J. Beebe, *Microfluidic logic gates and timers.* Lab on a Chip, 2007. **7**(11): p. 1449-1453.

32.   Rhee, M. and M.A. Burns, *Microfluidic pneumatic logic circuits and digital pneumatic microprocessors for integrated microfluidic systems.* Lab on a Chip, 2009. **9**(21): p. 3131-3143.

33.   Anandan, P., S. Gagliano, and M. Bucolo, *Computational models in microfluidic bubble logic.* Microfluidics and Nanofluidics, 2015. **18**(2): p. 305-321.

34.   Cartas-Ayala, M.A., et al., *Oscillations in light-triggered logic microfluidic circuit.* Microsystem technologies, 2014. **20**(3): p. 437-444.

35.   Morgan, A.J.L., et al., *Simple fluidic digital half-adder.* arXiv preprint arXiv:1602.01084, 2016.

36.   Ainla, A., et al., *Electrical Textile Valves for Paper Microfluidics.* Advanced Materials, 2017.

37.   Vourdas, N., K. Dalamagkidis, and V. Stathopoulos, *Active porous valves for plug actuation and plug flow manipulation in open channel fluidics.* RSC Advances, 2015. **5**(126): p. 104594-104600.

38.   Vourdas, N., et al., *Droplet Mobility Manipulation on Porous Media Using Backpressure.* Langmuir, 2016. **32**(21): p. 5250−5258.

39.   Vourdas, N., K. Dalamagkidis, and V.N. Stathopoulos, *uVALVIT: A tool for droplet mobility control and valving.* MATEC Web of Conferences, 2016. **41**.

40.   Vourdas, N., C. Ranos, and V.N. Stathopoulos, *Reversible and dynamic transitions between sticky and slippery states on porous surfaces with ultra-low backpressure.* RSC Advances, 2015. **5**(42): p. 33666-33673.

41.   Vourdas, N., A. Tserepi, and V.N. Stathopoulos, *Reversible pressure-induced switching of droplet mobility after impingement on porous surface media.* Applied Physics Letters, 2013. **103**(11): p. 111602.

42.   Milionis, A., E. Loth, and I.S. Bayer, *Recent advances in the mechanical durability of superhydrophobic materials.* Advances in colloid and interface science, 2016. **229**: p. 57-79.

43.   Pretet, J., et al. *Narrow-channel effects in LOCOS-isolated SOI MOSFETs with variable thickness.* in *SOI Conference, 2000 IEEE International.* 2000. IEEE.

44.   Chang, C.-Y., et al., *Reduced reverse narrow channel effect in thin SOI nMOSFETs.* IEEE Electron Device Letters, 2000. **21**(9): p. 460-462.

45.   Vourdas, N., et al., *Plug actuation and active manipulation in closed monolithic fluidics using backpressure.* In press, 2018.